

# Energy and Exergy Investigation of a Multigeneration System Based on Solar and Geothermal Energy Sources

Ammar Jalal Abdulrazzaq Al-Tabatabaee | Iraj Mirzaee\* | Morteza Khalilian |

Department of Mechanical Engineering, Engineering Faculty, Urmia University, Urmia, Iran

\* Corresponding author, Email: i.mirzaee@urmia.ac.ir

#### Article Information

### Article Type

RESEARCH ARTICLE

#### **Article History**

RECEIVED: 11 Jul 2025 REVISED: 01 Oct 2025 ACCEPTED: 30 Oct 2025

Published Online: 01 Nov 2025

#### Keywords

Multigeneration system PVT Geothermal energy Efficiency

#### Abstract

The research focuses on evaluating the energetic and exergetic sights of a newly developed multigeneration system utilizing geothermal energy and PVT solar collectors to create electricity, cooling, heat, hydrogen, and fresh water. This setup includes an organic Rankine cycle, a single-effect absorption chiller, a heat pump, a RO desalination unit and a PEM electrolyzer. The EES software was utilized to analyze thermodynamic and various parameters. Findings indicate that the system achieves energetic and exergetic outcomes of 10.29% and 36.77%, respectively. The net power output of the system totals 2004.86 kW, primarily driven by the ORC turbine. In addition, the cooling system realizes energetic and exergetic COPs of 0.54 and 0.22 based on the specified hypothesis. The system generates hydrogen at a daily rate of 796.8 kg and freshwater at a rate of 5.52 kg/s. Exergy destruction rate analysis reveals that the organic Rankine cycle suffers the most significant exergy loss.

Cite this article: Al-Tabatabaee, A. J. A., Mirzaee, I., Khalilian, M. (2025). Energy and Exergy Investigation of a Multigeneration System Based on Solar and Geothermal Energy Sources. DOI: 10.22104/hfe.2024.7164.1320



© The Author(s). Publisher: Iranian Research Organization for Science and Technology (IROST) DOI: 10.22104/hfe.2024.7164.1320

# 1 Introduction

The usage of energy has been affected by climate change. The demand for cooling increases with higher air temperatures and humidity, leading to a rise in air conditioning usage [1]. Additionally, periods of drought result in higher demand for irrigation, especially during growing seasons. Without adaptation, it is projected that energy demand related to climate change will rise by 25-58% by approximately 2050 [2]. Socioeconomic factors significantly influence energy usage behavior. A larger population, improved standard of living, a stronger economy, and increased mobility in human society contribute to the growing global energy demand.

Recently, the increasing worldwide need for energy, especially electricity, coupled with escalating energy production expenses and environmental issues, has motivated the advancement of new technologies focused on energy conservation and minimizing greenhouse gas emissions. One of the innovative technologies that has emerged is combined cooling, heating, and power (CCHP) systems, as well as combined heat and power (CHP) systems. CCHP systems can provide both heating and cooling in addition to power generation using the produced heat. These systems generate power at the location of consumption by utilizing the primary drive, distinguishing them from traditional power plants where a significant amount of fuel energy is lost as heat and energy losses during power transmission and distribution cannot be overlooked. Systems known as multigeneration systems are innovative systems that generate three or more outputs using one or more input energies.

Gupta and colleagues [3] conducted a study on developing a renewable energy system that involved an organic Rankine cycle combined with a triple pressure surface absorption system and a linear parabolic solar collector. The research focused on analyzing the impact of different input variables, including inlet pressure of turbine, solar radiation, outlet pressure of turbine, and ejector evaporator temperature, on the subsystems within the schematic. Heidarnejad and colleagues [4] focused on enhancing the proficiency of a geothermal power facility by incorporating biomass to generate sustainable electricity and potable water. Their findings indicated that the system could achieve energetic and exergetic efficiencies of 13.9% and 19.4% and that the total system cost was approximately 285.3\$ per hour. In their research, Assareh and colleagues [5] investigated a sustainable energy system that utilized geothermal and solar energy, along with thermoelectric generators, to supply electricity, cooling, and freshwater. Their detections proved that replacing condensers with thermoelectric generators resulted in a decrease in overall costs and an improvement in system efficiency. Following optimization, an exergy efficiency of 20.52% received and the final cost rate was determined to be 10.41 dollars per gigajoule. Alirahmi and Assareh [6] performed a study involving energy analysis, exergy, multi-objective optimization, and economic evaluation for a sophisticated energy production system aimed at generating electricity, freshwater, hydrogen, cooling and heating for the city of Dezful. They applied an optimization algorithm to enhance the objective functions. Their outcomes proved that the system's exergy efficiency stands at 31.66%, with a total unit cost of 21.9\$ per gigajoule (GJ).

In their research, Dezhdar et al. [7] concentrated on optimization, modeling, and exergoeconomic analysis of a multi-source energy production system that utilizes wind, solar energy, and ocean thermal energy in coastal areas. After optimizing the system, their outcomes indicated that the maximum exergy efficiency achieved is 14.47%, and the cost rate is 74.97\$ per hour. In their study, Boroomand et al. [8] examined the integration of the Brayton cycle and a central receiver solar collector system to generate fresh water, electricity, and cooling. Key factors considered in the research included solar radiation intensity, the quantity of mirrors or solar heliostats, the input pressure for the Rankine cycle turbine, and the compressor pressure ratio.

Prajapati and Shah [9] conducted a study that examined a system for producing H<sub>2</sub> through a combination of geothermal and solar energy, which are the primary renewable energy sources. The researchers also carried out a comparative analysis of several GPPs, to investigate the production rates and costs of hydrogen. Mohammadi et al. [10] showed a new system that harnesses solar and geothermal energy across multiple generations. This innovative system produces cooling, heating, electricity, and freshwater. The optimization outcomes reveal that the system can get a total unit cost of products at 34.1 \$/GJ and an exergetic efficiency of 25.4%. Comparative analysis demonstrates that this system exhibits higher exergy efficiency when compared to systems reliant on a single energy source.

Upon reviewing previously published research, it appears that the PTC collector is predominantly utilized, while the PVT solar collector is infrequently employed. Given that the PVT solar collector can generate both electricity and heat concurrently, this study intends to explore the use of PVT solar collectors along with geothermal energy as the primary energy sources for various productions.

# 2 System Description and Modeling

The diagram in Figure 1 depicts the renewable energy system under investigation, utilizing solar and geother-

mal energy. This system comprises a heat pump, an organic Rankine cycle, an absorption refrigeration system, thermal energy storage, a PEM electrolyzer, and subsystems for reverse osmosis water desalination. It generates cooling, electricity, heating, fresh water, and hydrogen.

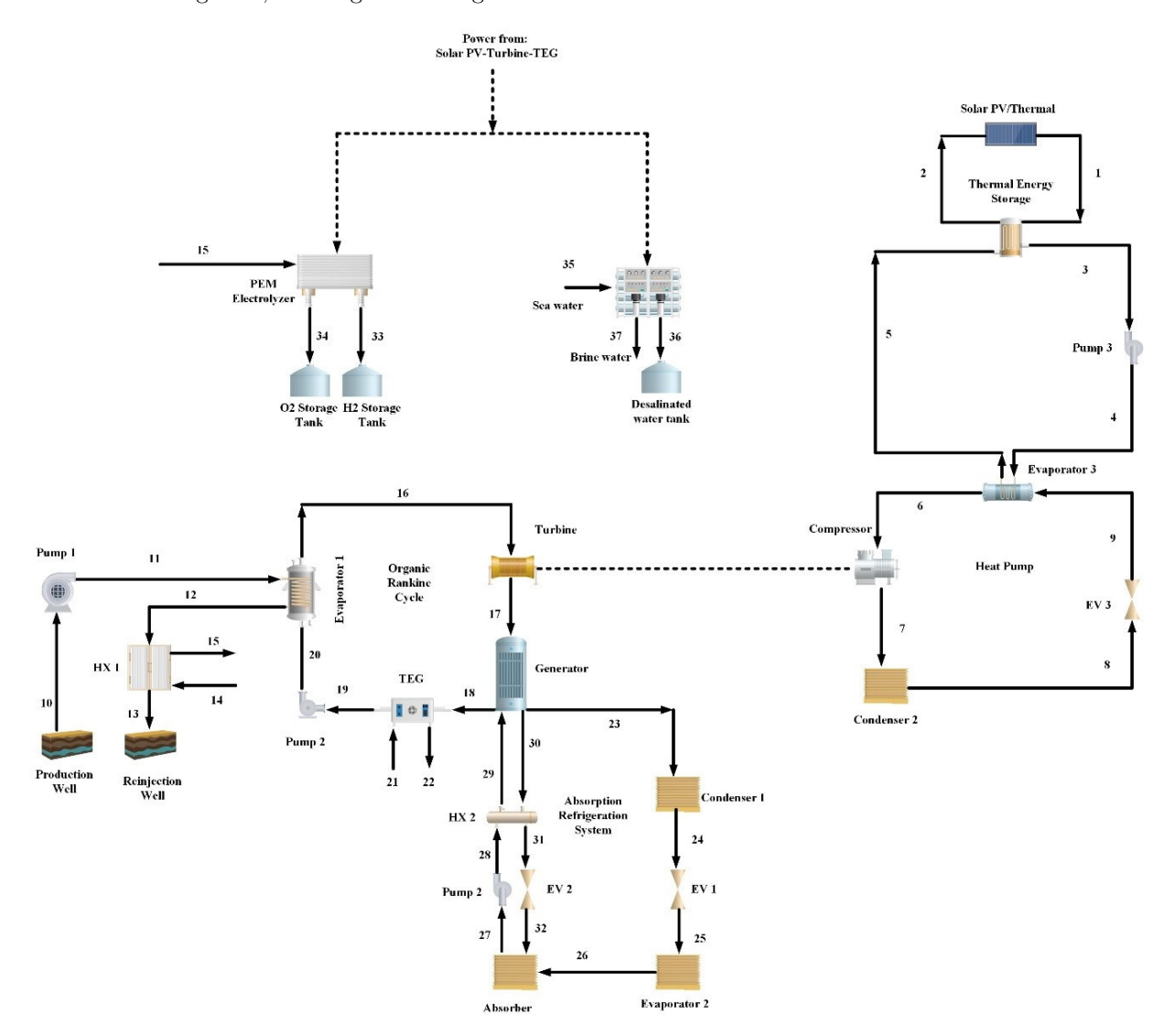


Fig. 1. The proposed multigeneration system.

The system diagram in Figure 1 illustrates an organic Rankine cycle in which working fluid is isobutane, powered by medium to high temperature geothermal water. The geothermal water comes out from the production well at point 10, passes through a pump, and subsequently enters the organic Rankine cycle's evaporator at point 11. After transferring its heat to the organic Rankine cycle, the fluid proceeds to heat exchanger 1 before reaching the reinjection well. Heat exchanger 1 serves the purpose of warming the wa-

ter utilized in the electrolysis process. The working fluid within the organic Rankine cycle is heated in the evaporator, moves to the turbine at point 16, and exits at point 17, where it releases heat to the generator of the absorption refrigeration system. To facilitate additional power generation, a TEG unit replaces the condenser in the organic Rankine cycle. Isobutane enters the TEG at point 18, progresses to the pump at point 19 to boost its pressure, and then re-enters the evaporator. The solar thermal system heats the water,

which is then stored in thermal energy reserves to guarantee a continuous operation of the heat pump for 24 hours. Since this system is set up in a residential area, the demand for heating, cooling, and electricity is consistent, necessitating operation every hour of every day. By harnessing geothermal energy along with a thermal energy storage system, it enables continuous production of power, cooling, heating, and hot water. The energy needed for this entire operation comes from the power generated by the organic Rankine cycle turbine, TEG unit, and the solar PV/T. This electricity is utilized for the PEM electrolyzer and the reverse osmosis desalination unit to generate hydrogen and freshwater.

The investigated system analysis is based on several assumptions:

- Compressors, expansion valves, pumps, and turbines function under adiabatic conditions.
- Hydrogen, air, and oxygen are regarded as ideal gases.
- The surrounding environmental conditions are 25 °C and a pressure of 100 kPa.
- Variations in potential and kinetic energy, as well as exergy components, are deemed negligible.
- Both the processes are in a steady state and exhibit steady flow.
- There is no chemical reaction occurring between the refrigerant and the absorbent; therefore, only physical exergy is considered while chemical exergy is disregarded.

The thermodynamic assessment has carefully investigated the equations related to mass balance, energy balance, the fundamental equations for energy and exergy efficiency, and also the exergy loss within the system.

$$\sum \dot{m}_{\rm in} - \sum \dot{m}_{\rm out} = \frac{dm_{\rm cv}}{dt}, \qquad (1)$$

$$\dot{Q} - \dot{W} + \sum_{\rm in} \dot{m}_{\rm in} \left( h_{\rm in} + \frac{V_{\rm in}^2}{2} + gZ_{\rm in} \right)$$

$$- \sum_{\rm in} \dot{m}_{\rm out} \left( h_{\rm out} + \frac{V_{\rm out}^2}{2} + gZ_{\rm out} \right) = \frac{dE_{\rm cv}}{dt}, \qquad (2)$$

$$\dot{\mathbf{E}}\mathbf{x}_Q + \sum_{in} \dot{m}_{in} \mathbf{e}\mathbf{x}_{in} = \sum_{out} \dot{m}_{out} \mathbf{e}\mathbf{x}_{out} + \dot{\mathbf{E}}\mathbf{x}_W + \dot{\mathbf{E}}\mathbf{x}_D, \quad (3)$$

The calculation of the power generated by the PV module will be performed in the following manner:

$$P_{\text{PVT}} = \eta_c \dot{I} \beta_c \tau_a A. \tag{4}$$

In this research, the efficiency of the solar cell  $(\eta_c)$  is 0.38, the packing factor  $(\beta_c)$  of the solar cell is 0.83, the transmittance of the solar panel glass  $(\tau_g)$  is 0.95, and A denotes the area of the solar collector measured in square meters. Consequently, the effective heat output

rate from the air collectors of the photovoltaic-thermal (PVT) system is demonstrated below.

$$\dot{Q}_{\text{PVT,solar}} = \frac{\dot{m}_{\text{air}} \text{Cp}_{\text{air}}}{U_L} \left[ (h_{p2z} Z \dot{I}) - U_L (T_{\text{air,in}} - T_0) \right] \times \left[ 1 - \exp\left(\frac{-bU_L L}{\dot{m}_{\text{air}} \text{Cp}_{\text{air}}}\right) \right], \tag{5}$$

$$A_{\text{PVT}} = \alpha_b \tau_q^2 (1 - \beta_c) + h_{p1G} \tau_g \beta_c (\alpha_c - \beta_c).$$
 (6)

The absorptivity of the solar cell, represented as  $\alpha_c$ , is 0.85, while the absorptivity of a surface, indicated as  $\alpha_b$ , is 0.9. In Equation (6), UL signifies the overall heat transfer coefficient from the solar cell to the surrounding environment via the top and back surfaces of the insulation, with a value of 4/71 W/m²K. The energy balance of the panel can be computed using the air outlet temperature from the PVT panel.

$$T_{\text{air,out}} = \left[ T_0 + \frac{h_{p2z}Z\dot{I}}{U_L} \right] \left[ 1 - \frac{1 - \exp(\frac{-bU_LL}{\dot{m}_{\text{air}}Cp_{\text{air}}})}{\frac{bU_LL}{\dot{m}_{\text{air}}Cp_{\text{air}}}} \right] + T_{\text{air,in}} \left[ \frac{1 - \exp(\frac{-bU_LL}{\dot{m}_{\text{air}}Cp_{\text{air}}})}{\frac{bU_LL}{\dot{m}_{\text{air}}Cp_{\text{air}}}} \right].$$
 (7)

The definition of the PVT collector's thermal efficiency will be as follow:

$$\eta_{\text{th,PVT}} = \frac{\dot{Q}_{\text{PVT}}}{\dot{I}bL} \,.$$
(8)

The solar intensity is indicated by  $(\dot{I}$ , while the dimensions of the PV/T panel are represented by b for width and L for length.

The energy and exergy balance equations for the studied multigeneration system detail the methods for determining the power and heat transferred, along with the exergy destruction rate for each eqyipment, as illustrated in Table 1.

# 3 Results and Discussions

Simulating the multigeneration system involves selecting specific parameters. Table 2 displays the input parameters for system modeling. The initial step in performing further calculations is to set these parameters.

Based on the original quantities, the EES [11] software is used to simulate the system, and the results from this simulated system are presented in Table 3.

In Figure 2, the rates of exergy destruction across various equipment of the system are presented. The findings indicate that the organic Rankine cycle and the PEM have the greatest rates of exergy loss.

Equipment	Energy balance equations	Exergy destruction rate equations
PV/T collector	$\dot{m}_2 h_2 + \dot{Q}_u = \dot{m}_1 h_1$	$\dot{\mathbf{E}}\dot{\mathbf{x}}_{D,\mathrm{PVT}} = \dot{\mathbf{E}}\dot{\mathbf{x}}_{\mathrm{sun}} + \dot{\mathbf{E}}\dot{\mathbf{x}}_{2} - \dot{\mathbf{E}}\dot{\mathbf{x}}_{1}$
TES	$\dot{Q}_{\rm TES} = U(T_1 - T_0)$	$\dot{\mathbf{E}}\mathbf{x}_{d,\mathrm{TES}} = \dot{\mathbf{E}}\mathbf{x}_1 - \dot{\mathbf{E}}\mathbf{x}_2 - \dot{\mathbf{E}}\mathbf{x}_Q$
Compressor	$\dot{W}_{\rm comp} = \dot{m}_6(h_7 - h_6)$	$\dot{\mathbf{E}}\mathbf{x}_{D,\text{comp}} = \dot{W}_{\text{comp}} + \dot{\mathbf{E}}\mathbf{x}_6 - \dot{\mathbf{E}}\mathbf{x}_7$
Condenser 2	$\dot{Q}_C = \dot{m}_7(h_7 - h_8)$	$\dot{\mathbf{E}}\dot{\mathbf{x}}_{d,C} = \dot{\mathbf{E}}\dot{\mathbf{x}}_7 - \dot{\mathbf{E}}\dot{\mathbf{x}}_8$
Pump 1	$\dot{W}_{p1} = \dot{m}_{10}(h_{11} - h_{10})$	$\dot{\mathbf{E}}\dot{\mathbf{x}}_{D,p1} = \dot{W}_{p1} - \dot{\mathbf{E}}\dot{\mathbf{x}}_{10} + \dot{\mathbf{E}}\dot{\mathbf{x}}_{11}$
Pump 2	$\dot{W}_{p2} = \dot{m}_{19}(h_{20} - h_{19})$	$\dot{\mathbf{E}}\dot{\mathbf{x}}_{D,p2} = \dot{W}_{p2} - \dot{\mathbf{E}}\dot{\mathbf{x}}_{19} + \dot{\mathbf{E}}\dot{\mathbf{x}}_{20}$
Pump 3	$\dot{W}_{p3} = \dot{m}_{27}(h_{28} - h_{27})$	$\dot{\mathbf{E}}\dot{\mathbf{x}}_{D,p3} = \dot{W}_{p3} - \dot{\mathbf{E}}\dot{\mathbf{x}}_{27} + \dot{\mathbf{E}}\dot{\mathbf{x}}_{28}$
Pump 4	$\dot{W}_{p4} = \dot{m}_3(h_4 - h_3)$	$\dot{\mathbf{E}}\mathbf{x}_{D,p4} = \dot{W}_{p4} - \dot{\mathbf{E}}\mathbf{x}_3 + \dot{\mathbf{E}}\mathbf{x}_4$
HX1	$\dot{Q}_{\rm HX1} = \dot{m}_{12}(h_{12} - h_{13}) = \dot{m}_{15}(h_{15} - h_{14})$	$\dot{\text{Ex}}_{D,\text{HX}1} = \dot{\text{Ex}}_{12} + \dot{\text{Ex}}_{14} - \dot{\text{Ex}}_{13} - \dot{\text{Ex}}_{15}$
ORC evaporator	$\dot{Q}_{\text{eva,ORC}} = \dot{m}_{11}(h_{11} - h_{12}) = \dot{m}_{16}(h_{16} - h_{20})$	$\dot{\text{Ex}}_{D,\text{eva,ORC}} = \dot{\text{Ex}}_{11} + \dot{\text{Ex}}_{20} - \dot{\text{Ex}}_{12} - \dot{\text{Ex}}_{16}$
ORC turbine	$\dot{W}_{t, \mathrm{ORC}} = \dot{m}_{16}(h_{16} - h_{17})$	$\dot{\mathrm{Ex}}_{D,t,\mathrm{ORC}} = \dot{\mathrm{Ex}}_{16} - \dot{W}_{t,\mathrm{ORC}} - \dot{\mathrm{Ex}}_{17}$
ORC TEG	$\dot{Q}_{\mathrm{TEG,ORC}} = \dot{m}_{18}(h_{18} - h_{19}) = \dot{m}_{21}(h_{22} - h_{21})$	$\dot{\text{Ex}}_{D,\text{TEG,ORC}} = \dot{\text{Ex}}_{18} + \dot{\text{Ex}}_{21} - \dot{\text{Ex}}_{19} - \dot{\text{Ex}}_{22}$
ARS Generator	$\dot{Q}_{\mathrm{ARS},G} = \dot{m}_{15}(h_{16} - h_{15})$	$\dot{\text{Ex}}_{d,ARS,G} = \dot{\text{Ex}}_{17} + \dot{\text{Ex}}_{29} - \dot{\text{Ex}}_{18} - \dot{\text{Ex}}_{23} - \dot{\text{Ex}}_{30}$
ARS Condenser	$\dot{Q}_{\mathrm{ARS},C} = \dot{m}_{23}(h_{23} - h_{24})$	$\dot{\mathrm{Ex}}_{d,\mathrm{ARS},C} = \dot{\mathrm{Ex}}_{23} - \dot{\mathrm{Ex}}_{24}$
ARS Evaporator	$\dot{Q}_{ m ARS,eva} = \dot{m}_{26}(h_{26} - h_{25})$	$\dot{\mathrm{Ex}}_{d,\mathrm{ARS,eva}} = \dot{\mathrm{Ex}}_{25} - \dot{\mathrm{Ex}}_{26}$
ARS Absorber	$\dot{Q}_{ m ARS,abs} = \dot{m}_{26}h_{26} + \dot{m}_{32}h_{33} - \dot{m}_{27}h_{27}$	$\dot{\mathbf{E}}\dot{\mathbf{x}}_{d,\mathrm{ARS,abs}} = \dot{\mathbf{E}}\dot{\mathbf{x}}_{26} + \dot{\mathbf{E}}\dot{\mathbf{x}}_{32} + \dot{\mathbf{E}}\dot{\mathbf{x}}_{27}$
ARS HX	$\dot{Q}_{\text{ARS,HX2}} = \dot{m}_{30}(h_{30} - h_{31}) = \dot{m}_{28}(h_{29} - h_{28})$	$\dot{E}\dot{x}_{d,ARS,HX1} = \dot{E}\dot{x}_{28} + \dot{E}\dot{x}_{30} - \dot{E}\dot{x}_{29} - \dot{E}\dot{x}_{31}$
PEM	$\dot{W}_{ ext{PEM}} = (\dot{m}_{15}h_{15} - \dot{m}_{33}h_{33} - \dot{m}_{34}h_{34})$	$\dot{\text{Ex}}_{D,\text{PEM}} = \dot{\text{Ex}}_{15} + \dot{W}_{\text{PEM}} - \dot{\text{Ex}}_{33} - \dot{\text{Ex}}_{34}$
RO	$\dot{W}_{\mathrm{RO}} = (\dot{m}_{35}h_{35} - \dot{m}_{36}h_{36} - \dot{m}_{37}h_{37})$	$\dot{\text{Ex}}_{D,RO} = \dot{\text{Ex}}_{35} - \dot{\text{Ex}}_{36} - \dot{\text{Ex}}_{37}$
СОР	$ ext{COP}_{ ext{en}} = rac{\dot{Q}_{ ext{ARS,eva}}}{\dot{Q}_{ ext{ARS},G}}$	
	$\text{COP}_{\text{ex}} = \frac{\dot{Q}_{\text{ARS,eva}} (1 - \frac{T_0}{T_{\text{eva}}})}{\dot{Q}_{\text{ARS,}G} (1 - \frac{T_0}{T_C}) + \dot{W}_{\text{net,ARS}}}$	

Table 1. Energy balance equations and rates of exergy destruction for every component of the suggested system.

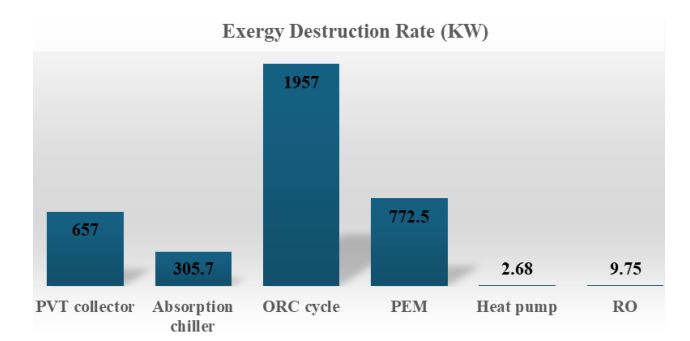


Fig. 2. The exergy destruction rate varies in different sections of the system.

The relationship between the size of the PVT solar collector and the amount of power and heat it produces is illustrated in Figure 3. There is a direct correlation between the collector's area and the power and heat it generates. Therefore, as the area increases, the solar collector absorbs more solar energy. The graphs indicate that when the PVT area increases from  $50\,\mathrm{m}^2$  to  $150\,\mathrm{m}^2$ , the heat produced changes from  $300.7\,\mathrm{kW}$  to  $902\,\mathrm{kW}$ , and the power produced changes from  $34.74\,\mathrm{kW}$  to  $104.2\,\mathrm{kW}$ .

In Figure 4, the effects of rising PVT solar radiation on the efficiencies of the proposed solar system are presented. The figure displays that as solar irradiance increases, both the energetic and exergetic efficiencies of the solar energy system decline, since the energy yield of the solar module rises at a slower rate than the increase in solar irradiance. The graphs reveal that changing the solar irradiation from  $500\,\mathrm{W/m^2}$  to  $1000\,\mathrm{W/m^2}$  leads to a 42.18% variation in energetic efficiency and a 48.7% reduction in exergetic efficiency. This illustrates that changes in solar radiation received by the PVT solar collector significantly affect the energetic and exergetic outcomes of the solar system.

Table 2. Parameters for the current study's modeling.

Parameters	Unit	Value			
	PV/T	. 5.240			
Dimensions	m	$1.31 \times 2.175 \times 0.18$			
Area	$m^2$	2.85			
Cell dimensions	m	$0.125 \times 0.125$			
Highest temperature	$^{\circ}\mathrm{C}$	< 134			
Sun Temperature	$^{\circ}\mathrm{C}$	5800			
Solar radiation					
intensity	$W/m^2$	800			
PV/T modules total	,				
area	$m^2$	85			
	Ieat Pump				
		outane			
Working fluid: Isobutane Turbine inlet					
temperature, $T_6$	$^{\circ}\mathrm{C}$	9.5			
Turbine outlet	Ü	0.0			
temperature, $T_7$	$^{\circ}\mathrm{C}$	75			
Compressor	Ü	. •			
isentropic efficiency	%	85			
	RO				
Recovery ratio, RR	-	0.3			
Number of elements,		0.0			
$n_e$	_	7			
Number of pressure		'			
vessels, $n_v$	_	42			
Seawater salinity, $X_f$	g/kg	43			
Seawarer sammey, 11j	ORC				
Working	g fluid: Isol	outane			
Turbine inlet	,				
temperature, $T_{16}$	$^{\circ}\mathrm{C}$	145			
Turbine inlet	Ü	110			
pressure, $P_{16}$	kPa	1500			
Isentropic efficiency					
of the turbine	%	85			
Isentropic efficiency	, 0				
of the pump	%	80			
Absorption refrigeration system					
Temperature of					
evaporator, $T_{\text{eva}}$	$^{\circ}\mathrm{C}$	5			
Temperature of					
condenser, $T_{\rm con}$	$^{\circ}\mathrm{C}$	40			
Temperature of					
absorber, $T_{\rm abs}$	$^{\circ}\mathrm{C}$	35			
Temperature of					
generator, $T_{\text{des}}$	$^{\circ}\mathrm{C}$	100			
garrantar, rucs	PEM				
$P_{\mathrm{H}_2}, P_{\mathrm{O}_2}$	atm	1			
$T_{\text{PEM}}$	$^{\circ}\mathrm{C}$	80			
$E_{\text{act},a}$	kJ/mol	76			
$E_{\mathrm{act},c}$	kJ/mol	18			
$\lambda_a$	-	14			
$\lambda_c$	_	10			
D	$_{ m mm}$	50			
$J_a^{ m ref}$	$A/m^2$	$1.7 \times 10^{5}$			
$J_c^{a}$	$A/m^2$	$4.6 \times 10^3$			
~ c	,	2.0 // 10			

Table 3. The overall thermodynamic efficiency of the system.

Parameters	Unit	Value
$\eta_{ m en}$	%	10.29
$\eta_{\mathrm{ex}}$	%	36.77
$Q_{\mathrm{PTV}}$	kW	511.1
$W_{t, ORC}$	kW	1834
$\dot{W}_{\mathrm{TEG}}$	kW	111.8
$\dot{W}_{ m net}$	$_{ m kW}$	2004.86
$P_{\mathrm{PVT}}$	kW	59.06
$COP_{en}$		0.54
$COP_{ex}$		0.22
$Q_{\text{cooling}}$	$_{ m kW}$	421.7
$\dot{m}_{ m H_2}$	kg/day	796.8
$\dot{m}_{ m Freshwater}$	kg/s	5.52
$\dot{\mathrm{Ex}}_{d,\mathrm{tot}}$	kW	5266

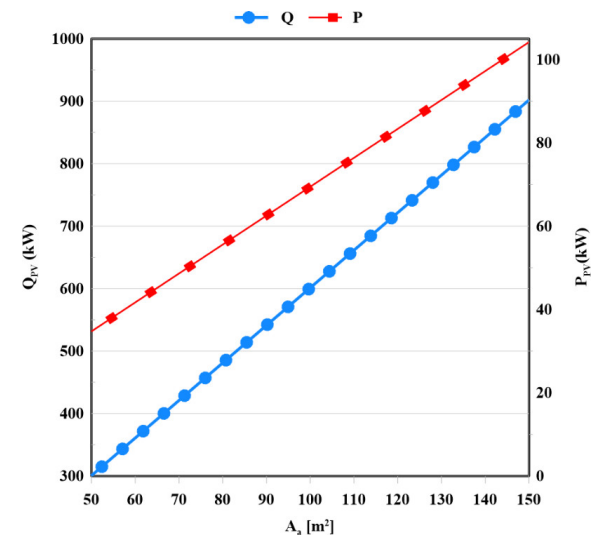


Fig. 3. The impact of the PVT solar collector total area on the amount of heat and power produced by the PVT collector.

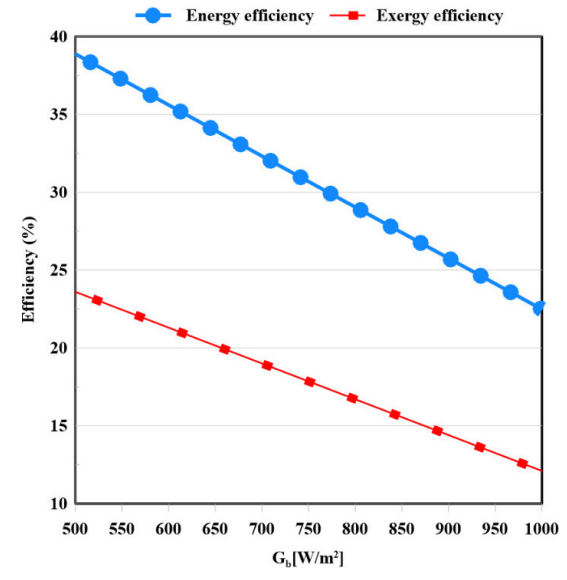


Fig. 4. The impact of PVT solar radiation on the solar system's energy and exergy efficiencies.

Many thermodynamic systems depend on the surrounding temperature for optimal operation. Consequently, variations in ambient temperature can either enhance or diminish the efficiency of the system. Figures 4 to 8 depicts how changes in ambient temperature affect the energetic and exergetic Coefficients of Perfor-

mance (COP) of the multigeneration system. As shown in Figure 5, an increase in ambient temperature results in no change to the energetic COP of the absorption cooling system. However, the exergetic COP of the absorption chiller experiences a marked rise from 0.15 to 0.649.

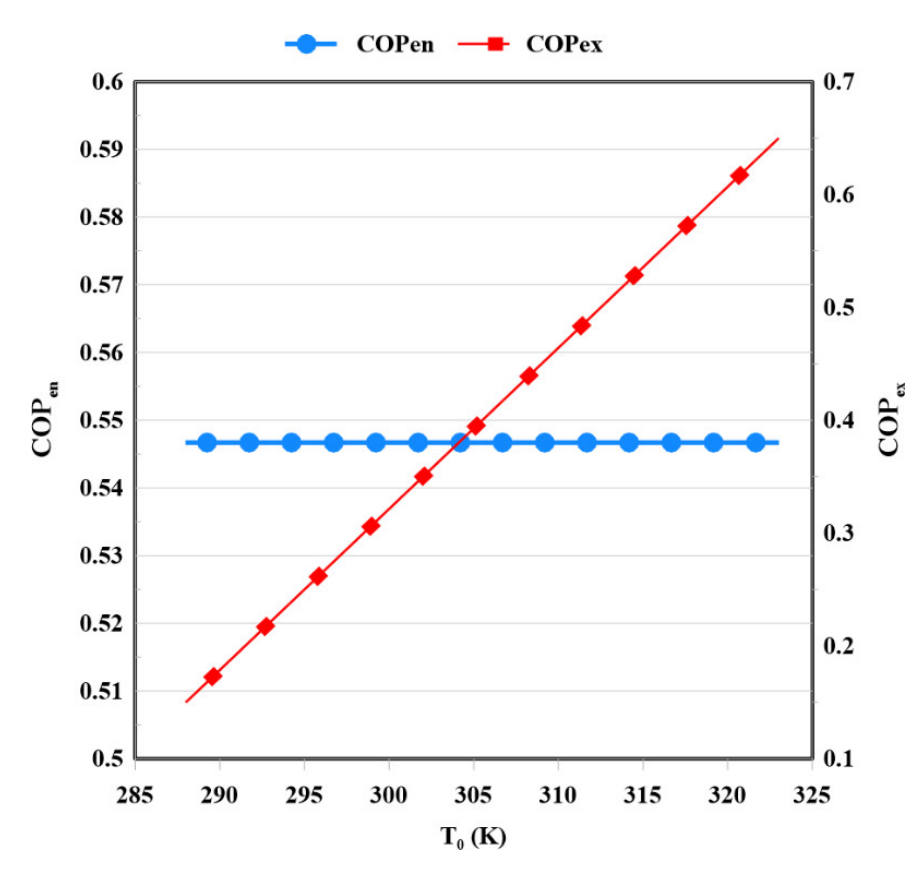


Fig. 5. Variation in the coefficient of performance (COP) of absorption cooling systems as ambient temperature increases.

The system is affected by two distinct inputs: solar energy and geothermal energy. The mass flow rates of these inputs play a vital function in the overall performance of the system. Figure 6 displays that an increase in the mass flow rate of geothermal water will reduce the efficiency of the organic Rankine cycle. This proves that the rise in power output will be significantly less than the rise in power input. When the geothermal fluid mass flow rate was altered from  $25~{\rm kg/s}$  to  $50~{\rm kg/s}$ , the energy efficiency dropped from 31.5% to 15%, while the exergy efficiency fell from 12.3% to 3.3%.

An increase in the mass flow rate of water in the solar energy system results in a decline in both energy and exergy outcomes for the entire system displayed in Figure 7. This occurs because the water mass flow rate is one of the two essential inputs for the overall system.

As a result, the total exergy efficiency drops from 6.3% to 6.18%.

The coefficient of performance (COP) serves as a common metric for appraising the efficiency of cooling systems. A variety of factors can influence a system, with the evaporator temperature being a critical aspect of cooling performance. Figure 8 indicates the energy and exergy COPs of the absorption chiller. An increase in the evaporator temperature leads to an enhancement in the energy COP of the cooling system, while the exergy COP declines. This is mainly due to the possible rise in heat input for the condenser at elevated temperatures, which boosts the energy efficiency of the system. Specifically, modifying the evaporative temperature from 275 K to 285 K can cause the energetic COP to change from 0.545 to 0.549.

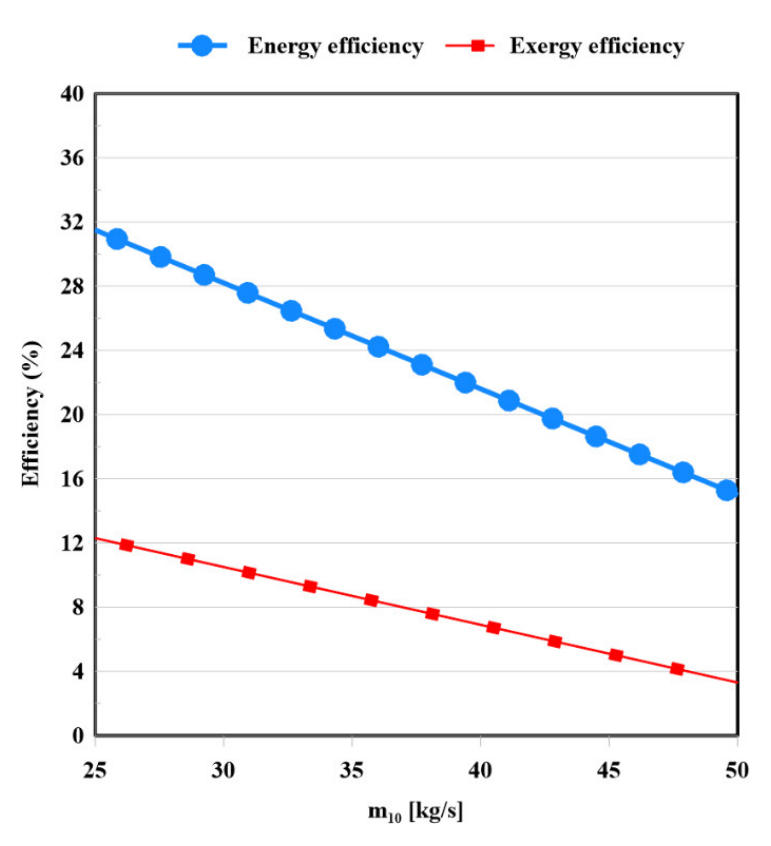


Fig. 6. The efficiency of the organic Rankine cycle changes as the geothermal water mass flow rate varies.

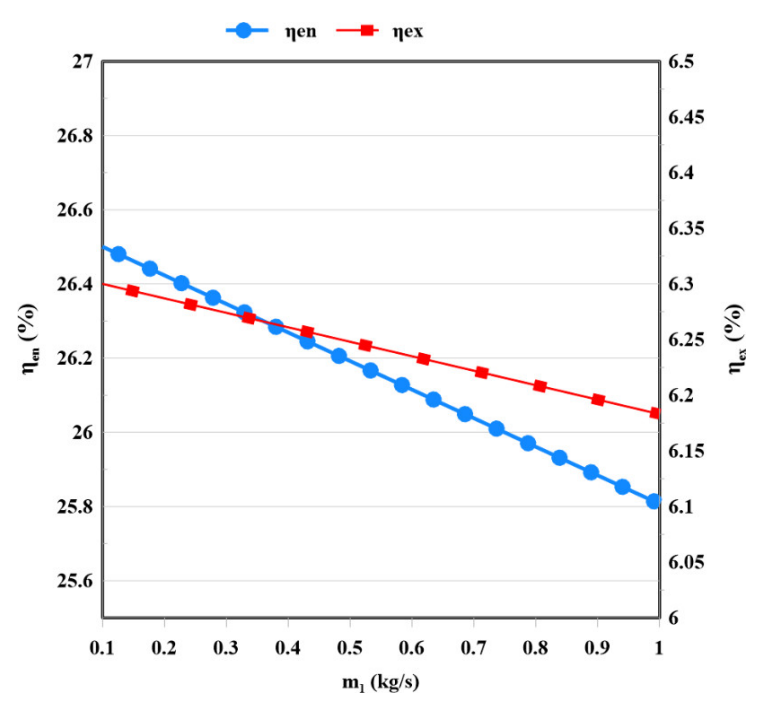


Fig. 7. Variation in the overall energy and exergy efficiencies as the water mass flow rate changes in a Solar PV/T system.

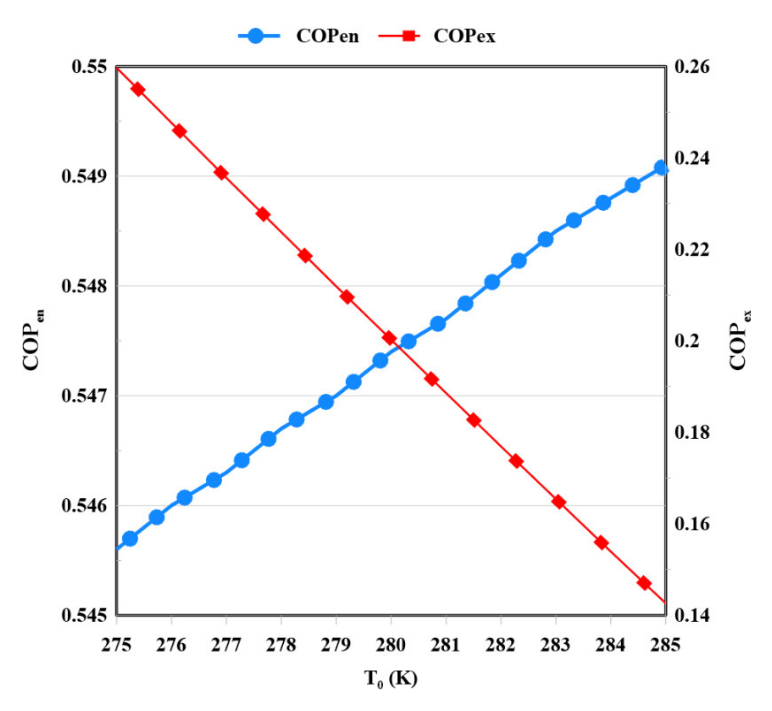


Fig. 8. The influence of varying evaporator temperature on the energetic and exergetic COPs of the cooling system.

# 4 Conclusions

The paper details the thermodynamic and thermoeconomic evaluation of a multigeneration system that can generate power, cooling, heat, hydrogen, and freshwater. This system is based on the organic Rankine cycle, single-effect absorption refrigeration system, heat pump, PEM electrolyzer, and RO unit. It employs two distinct energy sources: geothermal energy and the PVT collector, which serve as its main energy providers. The PVT solar collector is used for its capacity to generate both electricity and heat simultaneously, a topic that has been seldom explored in prior research. Initially, it presents the governing equations, as well as the thermodynamic and thermoeconomic equations for the proposed system. Then, the entire system is assessed using the EES software. The system's performance is analyzed, and the impressions of various parameters on its effectiveness are explored. The significant findings from the analysis and simulation of the system are as follows:

- Exergy destruction analysis in the primary cycles shows that the ORC cycle and PEM electrolyzer contribute most to the exergy destruction.
- A larger collector area and increased solar radiation of the solar collector led to higher system power generation.
- An increase in ambient temperature boosts the

- exergetic coefficient of performance (COP) without impacting the energetic COP.
- Elevated mass flow rates in both the geothermal and solar systems diminish energy and exergy outcomes.
- A rise in the evaporative temperature within the absorption system enhances the energetic COP of the refrigeration system, while simultaneously lowering the exergetic COP.

In terms of future research, it is recommended that this system be optimized for better efficiency, analyzed from the perspective of various ORC working fluids, and evaluated from an exergoeconomic standpoint.

## References

- Izadyar N, Miller W, Rismanchi B, Garcia-Hansen V, Matour S. Balcony design and surrounding constructions effects on natural ventilation performance and thermal comfort using CFD simulation: a case study. Journal of Building Performance Simulation. 2023;16(5):537–556.
- [2] Van Ruijven BJ, De Cian E, Sue Wing I. Amplification of future energy demand growth due to climate change. Nature communications. 2019;10(1):2762.

- [3] Gupta DK, Kumar R, Kumar N. Performance analysis of PTC field based ejector organic Rankine cycle integrated with a triple pressure level vapor absorption system (EORTPAS). Engineering Science and Technology, an International Journal. 2020;23(1):82–91.
- [4] Heidarnejad P, Genceli H, Asker M, Khanmohammadi S. A comprehensive approach for optimizing a biomass assisted geothermal power plant with freshwater production: Techno-economic and environmental evaluation. Energy Conversion and Management. 2020;226:113514.
- [5] Assareh E, Alirahmi SM, Ahmadi P. A Sustainable model for the integration of solar and geothermal energy boosted with thermoelectric generators (TEGs) for electricity, cooling and desalination purpose. Geothermics. 2021;92:102042.
- [6] Alirahmi SM, Assareh E. Energy, exergy, and exergoeconomics (3E) analysis and multi-objective optimization of a multi-generation energy system for day and night time power generation-Case study: Dezful city. International Journal of Hydrogen Energy. 2020;45(56):31555-31573.

- [7] Dezhdar A, Assareh Ea. Modeling, Optimization and exergoeconomic analysis a multiple energy production system based on solar Energy, Wind Energy and Ocean Thermal Energy Conversion (OTEC) in the onshore region. Journal of Energy Conversion. 2020;7(3).
- [8] Boroomand A, Assareh E. Hybrid of Brayton cycle and a Heliostat field collector (HFC) for Electricity, freshwater and cooling bar production. Journal of Energy Conversion. 2021;8(3):13–29.
- [9] Prajapati M, Shah M. Geothermal-solar hybrid systems for hydrogen production: A systematic review. International Journal of Hydrogen Energy. 2024;67:842–851.
- [10] Mohammadi M, Mahmoudan A, Nojedehi P, Hoseinzadeh S, Fathali M, Garcia DA. Thermoeconomic assessment and optimization of a multigeneration system powered by geothermal and solar energy. Applied Thermal Engineering. 2023;230:120656.
- [11] Klein SA. Engineering Equation Solver (EES) V9, F-Chart Software. Madison, USA; 2015.